

Experimental Physics 3: Experiment III

Compton scattering and gamma-ray attenuation

Group B

Andreas V. Flarup 202006446

Andreas S. Niebuhr 202005667

Rasmus L. Mikkelsen 202005762

Kristoffer I. R. Pedersen 202009792

IFA Aarhus University

Abstract

The aim of this experiment is to look at Compton scattering and find the distribution and energy of the scattered photon depending on the scattering angle in a BGO and NaI detector as well as finding the linear attenuation coefficient of aluminium and brass. The angle distribution of the scattered photon is found first. It is found to follow the theoretical curve well apart from a few data points and the overall tendency is clear. The energy of the scattered photon as a function of the angle is then found to fit even better, and the theoretical curve is not even fitted here. However the data points lie exactly on the theoretical curve, so maybe the errors were estimated too high. Lastly the attenuation coefficient of both aluminum and brass are found. They are found to be $\mu = (0.20 \pm 0.01)\text{cm}^{-1}$ for aluminium and $\mu = (0.65 \pm 0.03)\text{cm}^{-1}$ for brass. It is also seen that the intensity indeed is decaying exponential with depth in the materials.

1 Introduction

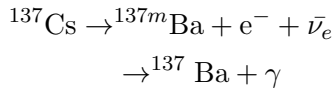
In this exercise ^{137}Cs sources are used to measure Compton scattering and gamma-ray attenuation. Compton scattering is an important scattering effect for photons as the discovery of Compton scattering was used to disprove that light can be explained as only a wave. This is because it's classical analogue, Thomson scattering, did not predict the effect to be significant at low intensities of X-ray. By not taking into account that electromagnetic waves consist of photons the theory simply did not agree with the experiments. Compton scattering is also important in different scientific fields such as radio-biology, as Compton scattering has a high chance of occurring when high energy photons interact with

matter. Gamma rays from the decay of nuclei have some highest photon energy, ranging from a few keV to a some MeV, making them very high energy particles. Since they have such a high energy, they can ionize atoms or molecules, making them very dangerous to life as they can easily go through and damage most organic material. However this can also be used as an advantage because it is possible to sterilize medical equipment or kill harmful bacteria in various food. Gamma rays are also very useful in nuclear medicine in imaging in for instance a PET scanning. [1] [2]. Firstly the angular distribution from the decay of a ^{137}Cs source will be measured as well as the energy of the scattered photon as a function of the scattered angle. Lastly the attenuation co-

efficient of gamma rays in aluminum and brass will be determined.

2 Theory

In the experiment the ^{137}Cs source is extremely important. It can decay, via a β^- decay, to



The emitted photon does not come from the ^{137}Cs source directly, but rather from the decay of the metastable ^{137m}Ba with a half-life of 2.552 ± 0.001 min. [3].

2.1 The detectors

We use two different detectors to scatter and detect the gamma rays and Compton radiation. Firstly we use a BGO (Bismuth Germanate) detector. The BGO material is dense[4], which means that there are a lot of electrons for our gamma rays to scatter on. The second detector was the NaI (Sodium Iodide). It has a very high efficiency, which gives us very accurate measurements, both for Compton scattered Photons and for measuring attenuation.[5] The detector is an inorganic scintillator, and it consists of only one crystal such that reflection and absorption at the faces are minimized. Since NaI is an insulator the valence band is almost full and the conduction band empty. The incoming photon can then excite an electron to the conduction band, and a photon will then be emitted when the electron falls down to the valence band again. Actually the detector is doped with Thallium such that states "inside" the band gap is created. This increases the probability of emitting a photon and also reduces self-absorption [6].

2.2 Compton Scattering

Compton scattering is when an incoming photon γ scatters on an electron in the target, as can be seen in figure 1. This can be seen as a quantum mechanical analogy to an elastic collision in 2 dimensions in classical mechanics. The incoming photon has energy E_γ . After the scattering the energy is transferred to kinetic energy of the recoiling electron K and energy of the scattered photon E'_γ . Compton scattering is most dominant for energies in the interval of approximately 100keV to 10MeV depending of the size of the atoms [6].

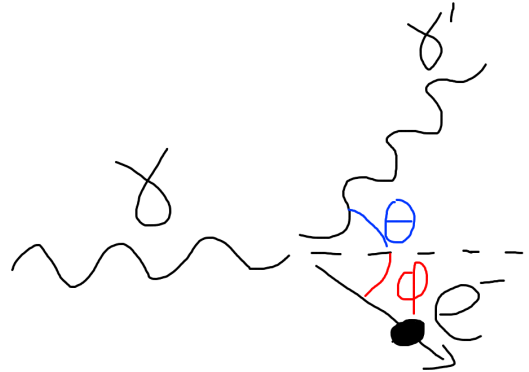


Figure 1: The scattered photon, γ' , moves at an angle θ relative to the incoming one. And the recoiling electron moves to the other side at an angle ϕ .

2.3 Conservation Equations

Assuming the target electron is at rest, energy conservation gives the relation

$$K = E_\gamma - E'_\gamma. \quad (1)$$

Here $E_\gamma = 661\text{keV}$ is the known energy of the incoming photon. Furthermore we demand conservation of momentum which gives the relations

$$p'_\gamma \sin \theta = p_e \sin \phi \quad (2)$$

$$p_\gamma = p_e \cos \phi + p'_\gamma \cos \theta, \quad (3)$$

where $p_\gamma = E_\gamma/c$ is the momentum of the incoming photon, $p'_\gamma = E'_\gamma/c$ is the outgoing photon's momentum.

$$p_e = \frac{1}{c} \sqrt{K^2 + 2Km_ec^2}$$

is the recoiling electron's momentum. K will in this experiment be between 200keV and 600 keV which is comparable to its rest energy $E_0 = m_ec^2 = 511\text{keV}$. Therefore it was important to use the relativistic formula for the energy [7].

$$\begin{aligned} K &= E_{tot} - m_ec^2 \\ &= \sqrt{(p_e c)^2 + (m_ec^2)^2} - m_ec^2 \end{aligned}$$

By using the constraints $K > 0$, $\phi, \theta \in (0, \pi)$, the quadratic formula and the identity $\sin(\arccos(x)) = \sqrt{1 - x^2}$ one can derive the formula $K(E'_\gamma)$ for conservation of momentum

$$\begin{aligned} K &= -m_ec^2 \\ &+ \sqrt{(m_ec^2)^2 + E_\gamma^2 + E'^2_\gamma - 2E_\gamma E'_\gamma \cos \theta} \end{aligned}$$

2.4 Photon Energy Dependence of Scattering Angle

From the conservation laws above, one can also obtain the relation

$$E'_\gamma = \frac{E_\gamma}{1 + E_\gamma/(m_ec^2)(1 - \cos \theta)}. \quad (4)$$

That again gives the relation between E_γ and E'_γ consistent with energy and momentum conservation [6]. m_e is the rest mass of the electron and c is the speed of light.

2.5 The Angular Distribution

The differential cross section $d\sigma/d\Omega$ is given by the Klein-Nishina formula [8]

$$\frac{d\sigma}{d\Omega} = \frac{1}{2} r_e^2 \left(\frac{\lambda}{\lambda'} \right)^2 \left[\frac{\lambda}{\lambda'} + \frac{\lambda'}{\lambda} - \sin^2(\theta) \right]$$

Where $\lambda = hc/E_\gamma$ is the wavelength of the incoming photon and vice versa with λ' . r_e is the classical electron radius such that

$$\frac{1}{2} r_e^2 = \frac{\alpha^2 \hbar^2}{2m_ec^2} \simeq 39.7\text{mb}.$$

However we are only interested in the relative cross-section, which then is given by

$$\frac{d\sigma}{d\Omega} = k \left[\left(\frac{E'_\gamma}{E_\gamma} \right)^3 + \frac{E'_\gamma}{E_\gamma} - \left(\frac{E'_\gamma}{E_\gamma} \right)^2 \sin^2 \theta \right] \quad (5)$$

Where k is a constant. Since E'_γ/E_γ is given by the θ dependence in equation 4 the only fit parameter is therefore k .

The number of photons r which scatter at an angle ω in a time interval Δt is

$$r = \Phi \Delta t \int_{\omega} \frac{d\sigma(\theta)}{d\Omega} d\Omega$$

Where Φ is the flux from the ^{137}Cs source. Since it can be assumed to be constant over the period of measuring, we see that the activity A at an angle θ has the distribution $\frac{d\sigma}{d\Omega}$. Here we absorb the relevant factors into k , and because we in practise measure over small solid angles where $\sigma(\theta)$ is almost constant, we expect the angular distribution measured in relative activities to follow equation 5.

2.6 Attenuation Coefficient

The attenuation coefficient describes how a beam of light is attenuated while penetrating a material. The intensity follows an exponential decay

$$I(z) = I_0 e^{-\mu z}$$

Which gives the expression for the attenuation coefficient μ to

$$\mu = \frac{\ln(I_0/I)}{z} \quad [9]. \quad (6)$$

where I_0 is the initial intensity, I is the intensity after going through the material and z is the distance that the beam has to go through the material. The coefficient dictates that the intensity is exponentially decreasing through the material. It is important to note, that the attenuation coefficient is also dependent on the energy of the photon.[9] In this report we will only look at a singular energy.

3 Experimental Setup

The experiment was conducted by using a BGO and a NaI detector to detect the decay from two ^{137}Cs sources. The goal of the experiment was to measure the angular distribution and the energy of the scattered photon as well as measuring the

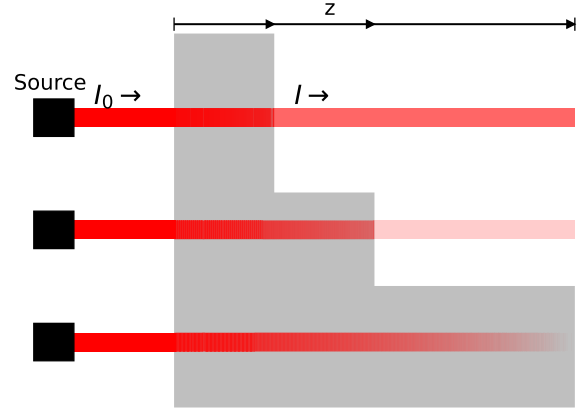


Figure 2: A demonstration of the attenuation of a light beam going through a material. A source is placed on the left side that gives a (in this case) collimated flux towards the right. The beam goes through the material and is attenuated by some amount depending on the thickness.

attenuation coefficient of gamma rays in different materials.

3.1 Channel to Energy Calibration

Firstly a channel to energy calibration is needed for the equipment. This was done by detaching the NaI detector from the movable arm and placing a point source in front of the detector. The different point sources used were ^{137}Cs , ^{226}Ra , and ^{133}Ba . Since the energy of the emitted photons were known it was possible to relate the channel number directly to the energy. These other sources were used as they emit photons in a range that is comparable with the photons from ^{137}Cs . As it was only relevant to see know where the energy peaked, the measurements lasted until

the expected peaks were clear to see which was about 5 min.

3.2 Angular Distribution

To measure the angular distribution of the scattered photon both the BGO and the NaI detectors were used as well as the strong ^{137}Cs source. The setup for the angular distribution can be seen on figure 3.

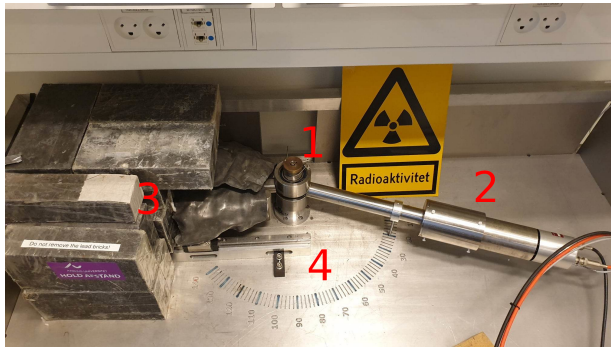


Figure 3: The strong ^{137}Cs source which is behind a lot of lead bricks, (3), sends out photons. The photons scatters in the BGO detector, (1), and then hits the NaI detector, (2). The NaI detector can be moved and the angle measured (4).

Both detectors are in use to make sure that only scattered photons are counted. Both detectors must detect a coincidence within a coincidence window, for it to be considered as a photon that is likely to have been Compton scattered. The coincidence window can be adjusted in the used software, Mc2Analyzer [10]. In the experiment the coincidence window was set to $0.2 \mu\text{s}$. The measurements must be done at different angles. In the experiment the measurements were done at 30° up to 116° at every 10th or 20th degree. The used angles can be seen in figure 7. The

time used for each measurement varied a lot and depended on which angle was measured at. At higher angles the detection rate was very low and lasted for 30 - 60 min. However the measurement at 116° lasted for 7.62h. At lower angles the detection rate was higher so these measurements lasted about 30 - 45 min.

3.3 Attenuation Coefficients

In this part of the experiment a different ^{137}Cs source is needed, the NaI detector is detached from the movable arm, and plates of aluminum and brass is used to measure the attenuation coefficient. The experimental setup is shown in figure 4.

Each of the aluminum plates were $1.0 \pm 0.05 \text{ cm}$ in width. Measurements were made with 1, 3, 5, and 7 aluminum plates. The measurements for aluminum lasted about 10 - 30 min. depending on the number of plates as the more material between the ^{137}Cs source and the detector, the fewer counts were measured. There were two brass plates: one with a width of 1.5 cm and one with a width of 3.0 cm. And the uncertainties were again estimated to $\pm 0.05 \text{ cm}$. However in both cases the uncertainty in thickness was negligible. And furthermore the uncertainty was randomly distributed or mostly due to the plastic caliber since we never got more than 0.05 cm of the estimated thickness times the number of plates. Measurements were made with $1.5 \pm 0.05 \text{ cm}$, $3.0 \pm 0.05 \text{ cm}$, and $4.5 \pm 0.05 \text{ cm}$ of brass. These measurements lasted for 10 - 20 min. depending on the amount of brass between the source and the detector.



Figure 4: The ^{137}Cs source, (2), sends photon through a little hole in the lead block, (4), which collimates the beam from the ^{137}Cs source. The beam passes through plates of a given material, (3), and then hits the NaI detector, (1).

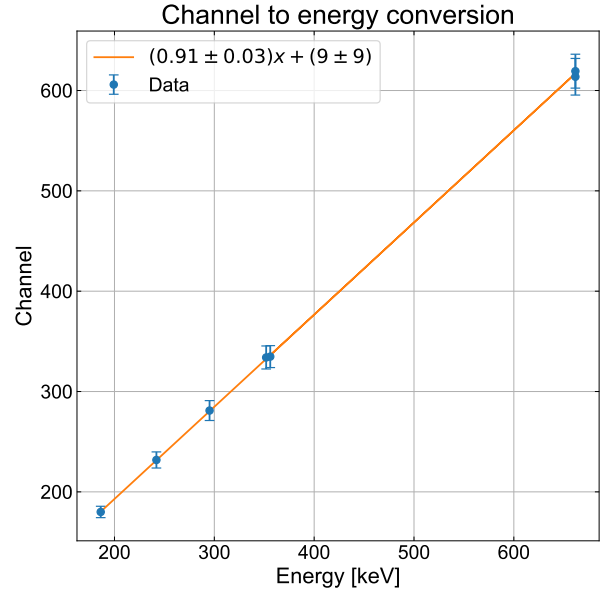


Figure 5: The relation follows a straight line very well, which justifies interpolation. The units on the slope is keV^{-1} and the offset is dimensionless (Channels).

4 Data

4.1 Channel to Energy Conversion

The channel to energy conversion was done by finding the peak in the spectrum of the different sources used, ^{137}Cs , ^{226}Ra , and ^{133}Ba . The reason why we chose these particular sources was that we just wanted to interpolate in the interval from approximately 200 keV to approximately 660 keV, and therefore wanted calibration measurements in this interval. A Gaussian was fitted around the peak to get the channel number corresponding to the peak. It is then possible to

correlate the channel number to the known emission energy of the different sources. This yielded the conversion seen on figure 5.

The fit gave the conversion rate $\text{channel} = (0.91 \pm 0.03)\text{keV}^{-1} \cdot E + (9 \pm 9)$. We used the computer algorithm "curve_fit" from the library "scipy.optimize" which makes weighted least squares fits with errors on the y-variable. But of course it is the inverse function that is of interest. So for the rest of the data analysis, the linear fit was inverted and the errors were propagated.

Angle [°]	Time [min]
30	32
40	27
50	45
60	67
80	46
90	26
100	53
116	457

Table 1: It was tried to increase the time length of the measurements at higher angles. However practical reasons sometimes made it impossible. On the other hand sometimes there was time for longer measurements at some random lower angles, which again was due to logistical reasons.

4.2 Finding Compton events

The measurements were done at the angles listed in table 1, and the time intervals were in general chosen longer at the higher angles in order to get enough Compton events.

To find the Compton scattering events, the conservation equations from section 2.3 are needed. As seen in figure 6 many events passed the time filter even though they could not be events from Compton scattering.

In order to use only the Compton events in the data analysis we drew an ellipse with center at the point which theoretically fulfilled both energy and momentum conservation. And only data points inside the ellipse were not filtered away. In order to make the comparison across the data sets at different angles, the area of the ellipses were held fixed. However, it was deformed differently since the spread of both energies decreased with lower energies. So as the set of Compton events moved up the line of energy conservation, the

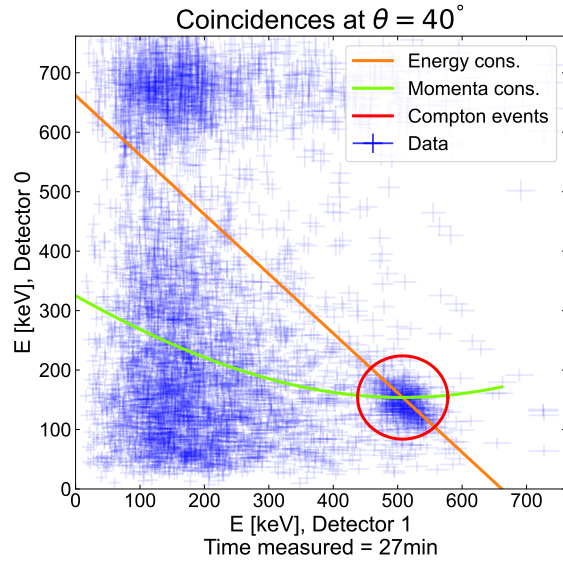


Figure 6: Example of a scatter plot (E'_γ, K) with uncertainties. Detector 1 (NaI) measured E'_γ and detector 0 (BGO) measured K . It is seen that there are many events registered near the predicted value for Compton scattering.

ellipse was stretched along the K axis. It is seen that there actually is a higher concentration of events around the predicted point from Compton scattering, which justifies the method and shows that we indeed have observed the Compton scattering effect. In practise we simply looked at the scatter plot and choose the shape such that the dens area around the theoretical point was within the ellipse. This was in general rather easy since the scatterplots revealed a clear border between background and the Compton events.

4.3 Angular Distribution

The results of the angular distribution can be seen on figure 7. The data points do follow the theoretical distribution in general (see equation 5). The fit was made with the function f given by

$$f(\theta) = \tilde{k} \left[\left(\frac{E'_\gamma}{E_\gamma} \right)^3 + \frac{E'_\gamma}{E_\gamma} - \left(\frac{E'_\gamma}{E_\gamma} \right)^2 \sin^2 \theta \right],$$

where E'_γ/E_γ is described on absolute scale as a function of θ in equation 4. \tilde{k} is a fitting constant containing k from equation 5, the flux of the source, Φ , and the solid angle, ω . The fit gave the value

$$\tilde{k} = (0.258 \pm 0.005)\text{s}^{-1}.$$

It is seen on the plot that one half of the points lie outside 1σ of the expected values. It is especially the angles $\theta = 50^\circ$ and $\theta = 116^\circ$ that contribute a lot to the χ^2 value being more than 3σ and 4σ outside the theoretical value. This gives the seemingly high numbers the $\chi^2 = 43$, $\chi^2/\nu = 6$ and the extremely bad p -value at $p = 4 \cdot 10^{-7}$. Here ν is the degrees of freedom. However the other data points match well and the decreasing tendency is clear anyway to at least second order in θ .

There are different effects one might suspect became relevant for the experiment. For instance, there was a background asymmetry with bands of higher intensity in the interval from 70 keV to 210 keV for E_1 and a band center around 660 keV for E_0 . Note that background in this case should be understood as radiation not coming from Compton scattering at the given angle the measurement was performed in.

This affected the measurements at the high angles as they came closer to the band and gave

asymmetric result as seen in figure 9. For the lower angles the background and it's asymmetry was very small, however, there was no significant correlation between angle size and the residual size of the data point.

4.4 Energy of Scattered Photon

The selected data points were collected in a histogram, and a Gaussian fit was made to find the energy and its uncertainty of the scattered photon E'_γ . An example is seen in figure 9. Finally, the measured energy of the scattered photon at different angles was collected as seen on figure 10. A theoretical curve can be calculated from equation 4, as the energy only depends on the variable θ , since everything else in the formula are known constants.

It is seen that the measurements follow the theoretical values very well. The p -value is $p = 1.00$ and $\chi^2 = 0.21$ giving $\chi^2/\nu = 0.03$ all indicating that the error bars might have been estimated way too high.

4.5 Attenuation Coefficients

To find the attenuation coefficients, depending on the length the gamma rays travel through, we first fitted a Gaussian around the peak of the spectrum of the decay of ^{137}Cs as seen on figure 11.

As seen in the figure the Gaussian is asymmetrical. This is due to the background being larger at lower energies than at higher. To remove the background a linear fit was made and the area under the linear fit was subtracted from the area of the Gaussian to only get the area between the orange and green functions on figure 11. This new Gaussian has the same height and standard

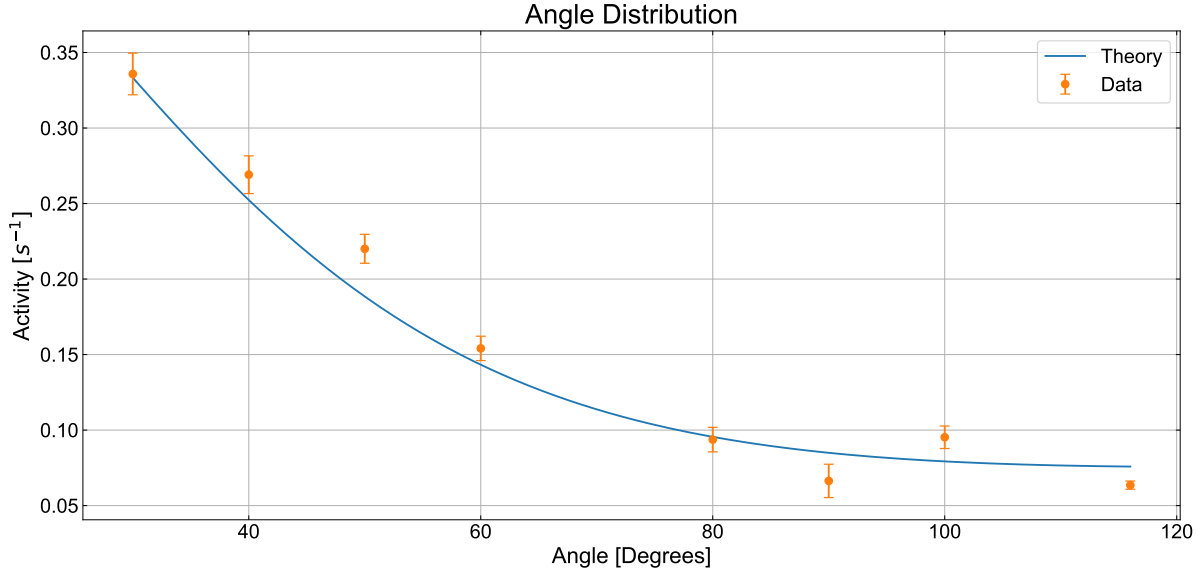


Figure 7: The angle distribution approximately follows the theory although half of the points does not lie on the theoretical curve within the uncertainties. The fitted curve comes from equation 5.

deviation as the original. The area was found and scaled with respect to time, as some of the measurements lasted longer than others. The errors were propagated and the result of the attenuation coefficient of aluminum can be seen on figure 12.

The measured attenuation coefficient for aluminum was found to be $\mu = (0.20 \pm 0.01)\text{cm}^{-1}$ for photons with an energy of 661 keV. The table value of the attenuation coefficient of aluminum at 662 keV photons is 0.20cm^{-1} [11].

For brass we found $\mu = (0.65 \pm 0.03)\text{cm}^{-1}$ as seen in figure 13. The found attenuation coefficient is at a photon energy of 661 keV.

5 Discussion

5.1 Angle Distribution

In general the measurement of the angle distribution matched the theory very well. The main reason for the bad numbers is namely isolated to the two measurements at $\theta = 50^\circ$ and $\theta = 116^\circ$. It is not clear why some of the angles are exceptional bad. For instance the background is increasing for lower E_γ and therefore at higher angles giving an asymmetric distribution in E_γ for the high angles as we saw in figure 9. However the problem with data points that deviate a lot from the theory does not seem to depend on the angle size. This actually indicates that the way we corrected for the background was successful in removing this systematic error. However this

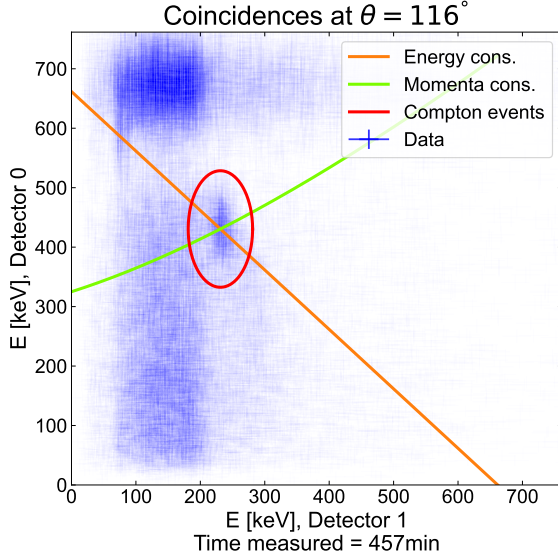


Figure 8: It is seen that the background radiation has bands of so high activity that a significant amount of it passes the coincidences window filter.

raises the question of what then courses the big fluctuations for some of the data points. It is also a possibility that there were no significant systematic errors in the experiment, but the method of calculating the uncertainties simply were a little too high. Should the experiment be done again, more measurements at more different angles could also give a better fit and maybe point towards a systematic error in the experiment.

5.2 Energy of Scattered Photon

The measurements of the energy of the scattered photon as a function of the scattering angle are all very good as all the measurements lie on the exact

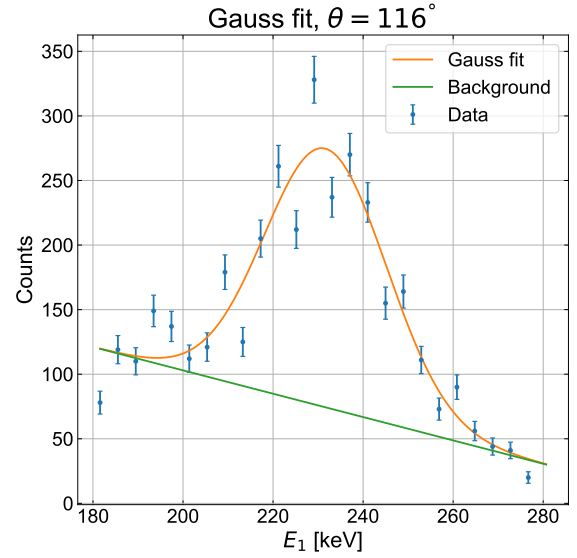


Figure 9: An example of a Gaussian fit to find E_γ . It is seen that the background is prominent and heeling at the very large angles.

theoretical curve 4 predicted with only absolute constants and no fitting constants. Therefore this can be seen as an indirect measurement of the relation between the fundamental coefficients in the formula; E_γ for the ^{137m}Ba decay, and the rest energy for the electron m_ec^2 . Of course this requires belief in the Compton scattering formula, but the results indicate a good reason for doing so. If one should be little more sceptical about the p -value at $p = 1.0$ and $\chi^2/\nu = 0.03$ this also suggests, that the uncertainties might have been estimated too high. These were calculated the usual way from the spread of the Gaussian fits which should be a fair way to do it. One could argue that this suggests that the way of selecting the data points with the ellipsis somehow broadens the peaks. However from just looking

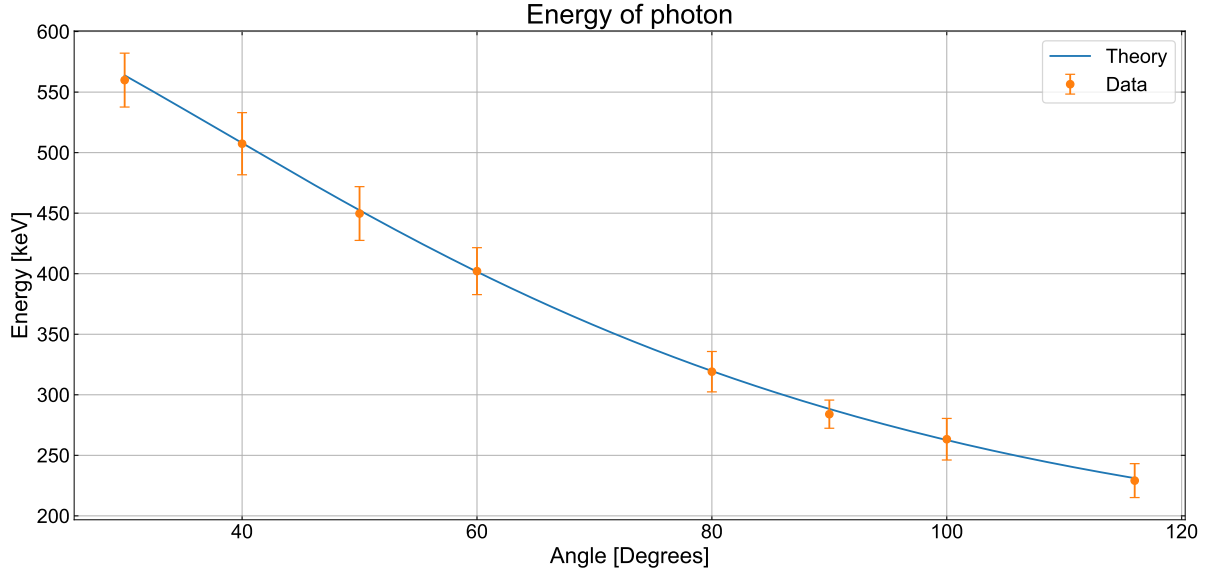


Figure 10: The energy of the scattered photon follows the theory very well. The theoretical curve is calculated exactly, as the energy of the scattered photon only depends on the variable θ , as seen in equation 4, since the rest are known constants.

at the densities of blue color in the scatter plots as in figure 6 one might estimate the uncertainties to be at the approximately same size. It would be interesting to perform the experiment again several times at the same angles to obtain empirical fluctuations and thereby errors. Hopefully this would either reveal some systematic errors at some of the angles or adjust the count rates and it's uncertainties.

5.3 Attenuation Coefficients

For aluminium the fit matched a straight line almost going through the origin. We actually got the theoretical value, so a goal for further study would be to reduce σ which we got to 5% of μ .

Here one should definitely measure more data points and also prioritise to measure for longer periods to decrease the uncertainties of the individual data points. This would be even more relevant for the brass part of the experiment since we here only had 3 data points. The offset was also so large here, that we could not estimate the uncertainties if we forced the fit through the origin. This indicates that there might have been a systematic error in this experiment. Maybe the two brass plates were not sufficiently identical. This could be fixed by getting more plates, and if one would investigate the differences between them you could try to measure at the same thicknesses z but with different plate constellations. This could also be a relevant method for the aluminium experiment to avoid systematical errors

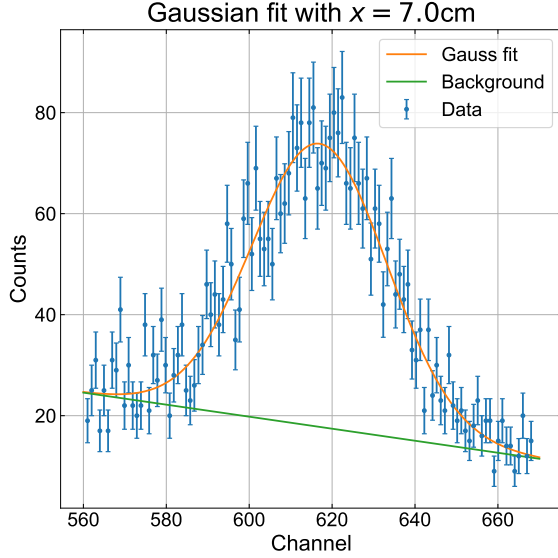


Figure 11: An example of a Gaussian fit to find the total counts with uncertainties for aluminum. Again it is seen that the background is heeling.

in the thickness differences. One might suspect that μ was not constant across the range, we measured. But this should also not be relevant since the heeled fit should be able to average this effect out anyway. And actually the measurement of the count rate with no plates also had the asymmetric background which indicates that this phenomena is caused by something else.

6 Conclusion

From the investigation of the angle distribution of the scattered photon we can conclude that the data generally follows the theoretical curve, but some of the data does not follow it exactly. Especially at the angles $\theta = 50^\circ$ and $\theta = 116^\circ$. New measurements at those angles as well as more

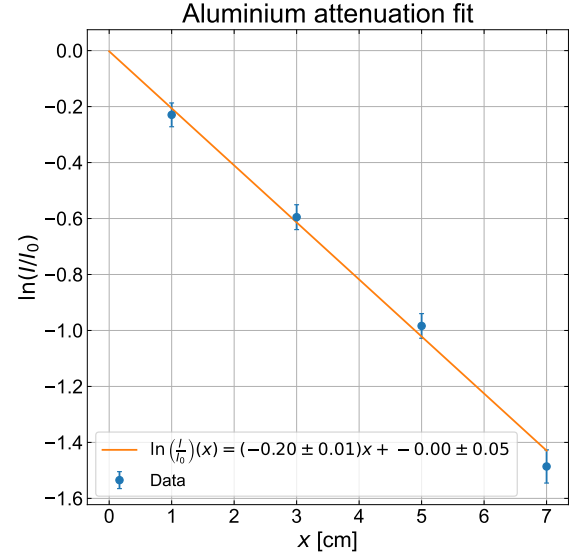


Figure 12: The data follows a straight line as expected see equation 2.6.

measurements at more angles could therefore be made to get a better fit if the experiment should be done again.

The energy of the scattered photon was found to follow the calculated theoretical curve well within the uncertainty band. However the uncertainties of the measurements seem to be high considering their position in relation to the theoretical curve. Therefore one should try to find a way to make the uncertainties smaller if the experiment should be performed again.

We measured the attenuation coefficient for aluminium to be $\mu = (0.20 \pm 0.01)\text{cm}^{-1}$ which was the table value. The measurement of brass gave the attenuation coefficient $\mu = (0.65 \pm 0.03)\text{cm}^{-1}$. The latter measurement had only 3 data points which makes room for a big improvement, if one could find more brass slices. The aluminium part

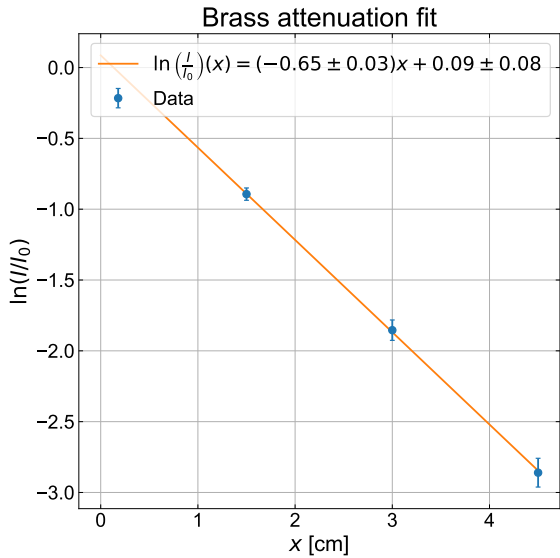


Figure 13: The data also follows a straight line see equation 2.6. However the offset is a little larger here.

could also benefit from having more data points to reduce the uncertainty further.

References

- [1] Compton scattering. URL: https://en.wikipedia.org/wiki/Compton_scattering.
- [2] Wikipedia - Gamma rays. URL: https://en.wikipedia.org/wiki/Gamma_ray.
- [3] Isotopes of Barium. URL: https://en.wikipedia.org/wiki/Isotopes_of_barium.
- [4] Luxium - BGO Scintillation Material. URL: <https://www.crystals.saint-gobain.com/radiation-detection-scintillators/crystal-scintillators/bgo-bismuth-germanate#>.
- [5] Luxium - NaI Scintillation Material. URL: <https://www.crystals.saint-gobain.com/radiation-detection-scintillators/crystal-scintillators/naitl-scintillation-crystals#>.
- [6] Kenneth S. Krane. *Introductory Nuclear Physics*.
- [7] Ulrik I. Uggerhøj. *Speciel relativitetsteori*.
- [8] Steven Weinberg. *The Quantum Theory of Fields (1995). Vol. I.* pp. 362–9.
- [9] Linear attenuation coefficient. URL: <https://radiopaedia.org/articles/linear-attenuation-coefficient>.
- [10] Guide to Mc2Analyzer. URL: <https://brightspace.au.dk/d2l/le/lessons/71471/topics/1015740>.
- [11] Efficiency Calculations. URL: <https://brightspace.au.dk/d2l/le/lessons/71471/topics/1015734>.